Properties of an α Particle in a Bohrium 270 Nucleus under the Generalized Symmetric Woods-Saxon Potential

Bekir Can LÜTFÜOĞLU [*1], **Muzaffer ERDOĞAN** [2]

[1]Akdeniz Üniversitesi, Fen Fakültesi, Fizik Bölümü, 07058, Antalya
[2]Namık Kemal Üniversitesi, Fen Edebiyat Fakültesi, Fizik Bölümü, 59030, Tekirdağ

Abstract: The energy eigenvalues and the wave functions of an α particle in a Bohrium 270 nucleus have been calculated by solving Schrödinger equation for Generalized Symmetric Woods-Saxon potential. Using the energy spectrum by excluding and including the quasi-bound eigenvalues, entropy, internal energy, Helmholtz energy, and specific heat, as functions of reduced temperature have been calculated. Stability and emission characteristics have been interpreted in terms of the wave and thermodynamic functions. The kinetic energy of a decayed α particle was calculated using the quasi-bound states, which has been found close to the experimental value.

Bir Bh-270 Çekirdeği İçinde Genelleştirilmiş Simetrik Woods-Saxon Potansiyeli Etkisindeki Bir α Parçacığının Özellikleri

Özet: Bir Boryum 270 çekirdeğinde bulunan bir α parçacığının enerji özdeğerleri ve dalga fonksiyonları, Schrödinger denklemi Genelleştirilmiş Simetrik Woods-Saxon potansiyeli için çözülerek hesaplanmıştır. Yarı bağlı durumları içeren ve içermeyen enerji spektrumları kullanılarak indirgenmiş sıcaklığın fonksiyonu olarak entropi, iç enerji, Helmholtz enerjisi ve özgül ısı hesaplanmıştır. Dalga ve termodinamik fonksiyonlar kullanılarak kararlılık ve ışınım karakteristikleri yorumlanmıştır. Yarı bağlı durum enerjileri kullanılarak bozunan bir α parçacığının kinetik enerjisi deneysel veri ile uyumlu olarak hesaplanmıştır.

1. Introduction

In the last decade, thermodynamic functions have been a subject of ongoing interest in understanding physical properties of potential fields in relativistic or non-relativistic regimes. Pacheco *et al.* has investigated Dirac oscillator in a thermal bath in one-dimension [1], then extended the study to three-dimensional case [2]. In these studies, for high temperatures, it has been reported that, in the one-dimensional case the heat capacity of the Dirac oscillator is twice as that of one-dimensional harmonic oscillator, while in the three-dimensional case, the limiting value of the specific heat capacity at high temperatures is three times greater than that of the one-dimensional case. Meanwhile, the first experimental one-dimensional Dirac oscillator has been studied by Franco-Villafañe *et al.* [3]. Boumali has used the Hurwitz zeta function to investigate the relativistic harmonic oscillator in thermodynamic point of view [4]. He has also calculated some thermodynamic functions of graphene under a magnetic field via the two-dimensional Dirac oscillator in an approach based on the zeta function [5]. On his following paper, Boumali has studied the thermal

properties of the one-dimensional Duffin-Kemmer-Petiau oscillator and computed the vacuum expectation value of its energy by using Hurwitz zeta function [6]. Arda *et al.* have studied some thermodynamic quantities of a linear potential in the Klein-Gordon equation with Lorentz vector and Lorentz scalar parts and for an inverse-linear potential, in Dirac equations with a Lorentz scalar term only. In both cases they have given the analytical results for high temperatures under the assumption of strong scalar potential term [7]. Dong *et al.* have exactly solved a one-dimensional Schrödinger equation of a harmonic oscillator with an additional inverse square potential by using operator algebra. They have studied the relations between the eigenvalues and eigenfunctions using a hidden symmetry and derived some of the thermodynamic functions of the system [8].

The Woods-Saxon Potential (WSP) [9] has been widely used in many areas of physics such as nuclear physics [9–16], atom-molecule physics [16, 17], relativistic [18–26] and non-relativistic [27–30] problems. In order to take the effects such as non-zero l, spin-orbit coupling, large

force suffered by nucleons near the surface of a nucleus, additional terms to WSP have been introduced to form various types of Generalized Symmetric Woods-Saxon Potential (GSWSP) [31–43]. GSWSP can be used to model any system, in which a particle is trapped in a finite space [44–48].

In this paper, we solve Schrödinger equation, substituting GSWSP for WSP to calculate the thermodynamic properties of an α particle in a Bohrium 270 nucleus, as an application of the formalism which has been studied in detail in [34].

Like WSP, the GSWSP does not possess analytical solutions for $l \neq 0$ cases. GSWSP serves our purpose for the case $l = 0$, which corresponds to spherical symmetry. This reduces the problem to one-dimensional form with the only radial degree of freedom.

In section 2, we first consider the GSWSP, and give the main result of [34], in section 3 we calculate the energy spectrum of an α particle employing the method given in the previous section. In subsection 3.1, we calculate partition functions using the energy spectra, then, Helmholtz free energies, internal energies, entropies and specific heat capacities of the system as functions of temperature. In section 4, our conclusion is presented.

2. Material and Method

Let us consider a nucleon under one-dimensional GSWSP [34];

$$
\begin{aligned}
V(x) &= \theta(-x)\left[-\frac{V_0}{1+e^{-a(x+L)}}+\frac{W_0 e^{-a(x+L)}}{\left(1+e^{-a(x+L)}\right)^2}\right] \\
&+ \theta(x)\left[-\frac{V_0}{1+e^{a(x-L)}}+\frac{W_0 e^{a(x-L)}}{\left(1+e^{a(x-L)}\right)^2}\right], \quad (1)
\end{aligned}
$$

here the second terms in the square brackets represent the energy barrier at the surface, which is linearly proportional to the spatial derivative of the first term and the radius. Thus the parameter W_0 is linearly proportional to a, L, V_0 and the proportionality constant can be determined by means of momentum and energy conservations for the nucleus under consideration. $\theta(\pm x)$ are the Heaviside step functions, V_0 is the depth of the potential given by [11]

$$
V_0 = 40.5 + 0.13A. \quad (2)
$$

We classify bound states to tight-bound and quasi-bound states since they obey different boundary conditions. In tight-bound case, the particles are confined in the well and they can have only negative energy eigenvalues. In other words their wave functions outside the well vanish. In quasi-bound case, although the particles are inside the potential well, they have positive energy eigenvalues and with appropriate conditions they can tunnel. Therefore their wave functions imply a propagation in outgoing direction from the potential well, contrary to tight-bound

states. Exploiting the continuity of the wave functions and their first spatial derivatives, as well behaved wave functions must obey, the quantization conditions are obtained. Moreover by using the $x \to -x$ symmetry of the potential well the energy spectrum can be given in two subsets as "even" and "odd" eigenvalues. In the reference [34] the energy eigenvalues for tight-bound states have been found as

$$
E_n^{tb-e} = -V_0 + \frac{\hbar^2}{2mL^2}\left|\arctan\frac{(N_1-N_2)}{i(N_1+N_2)}\pm n'\pi\right|^2, (3)
$$

$$
E_n^{tb-o} = -V_0 + \frac{\hbar^2}{2mL^2}\left|\arctan\frac{(N_1+N_2)}{i(N_1-N_2)}\pm n'\pi\right|^2, (4)
$$

while for quasi-bound states are

$$
E_n^{qb-e} = -V_0 + \frac{\hbar^2}{2mL^2}\left|\arctan\frac{(N_3-N_4)}{i(N_3+N_4)}\pm n'\pi\right|^2, (5)
$$

$$
E_n^{qb-o} = -V_0 + \frac{\hbar^2}{2mL^2}\left|\arctan\frac{(N_3+N_4)}{i(N_3-N_4)}\pm n'\pi\right|^2. (6)
$$

Here n' are integers, whereas n stands for the number of nodes, the roots of the wave functions. N_1, N_2, N_3, and N_4 are complex numbers

$$
N_1 = \frac{\Gamma(c_1)\Gamma(c_1-a_1-b_1)}{\Gamma(c_1-a_1)\Gamma(c_1-b_1)}, \quad (7)
$$

$$
N_2 = \frac{\Gamma(c_1)\Gamma(a_1+b_1-c_1)}{\Gamma(a_1)\Gamma(b_1)}, \quad (8)
$$

$$
N_3 = \frac{\Gamma(2-c_1)\Gamma(c_1-a_1-b_1)}{\Gamma(1-a_1)\Gamma(1-b_1)}, \quad (9)
$$

$$
N_4 = \frac{\Gamma(2-c_1)\Gamma(a_1+b_1-c_1)}{\Gamma(1+a_1-c_1)\Gamma(1+b_1-c_1)}, \quad (10)
$$

and implicitly dependent on the energy eigenvalues via the coefficients a_1, b_1 and c_1

$$
\begin{aligned}
a_1 &= \mu+\theta+\nu, & (11) \\
b_1 &= 1+\mu-\theta+\nu, & (12) \\
c_1 &= 1+2\mu, & (13)
\end{aligned}
$$

where

$$
\mu = \sqrt{-\frac{2mE_n}{a^2\hbar^2}}, \quad (14)
$$

$$
\nu = \sqrt{-\frac{2m(E_n+V_0)}{a^2\hbar^2}}, \quad (15)
$$

$$
\theta = \frac{1}{2}\mp\sqrt{\frac{1}{4}-\frac{2mW_0}{a^2\hbar^2}}. \quad (16)
$$

3. Results

In this manuscript we investigate an α particle in a heavy nucleus, Bohrium 270. a, the reciprocal of the diffusion parameter, is taken to be $a = 1.538 fm^{-1}$ [11] and the nuclear radius is calculated as $L = 8.068 fm$. Then we substitute the atomic number $A = 270$ of the nucleus, and

find out $V_0 = 75.617 MeV$ and $W_0 = 215.523 MeV$. In Figure 1, the GSWSP is shown.
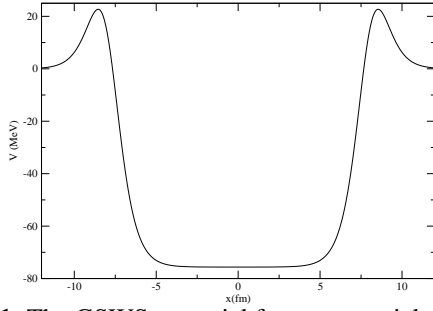
Figure 1. The GSWS potential for an α-particle in a Bohrium 270 nucleus.

The tight-bound energy eigenvalues calculated via Equation 3 and Equation 4 fall into the interval such that,

$$-V_0 < E_n^{tb} < 0, \tag{17}$$

are presented in Table 1.

Table 1. The tight-bound energy spectrum of the α particle confined in Bohrium 270 nucleus.

n	$E_n^{tb}(MeV)$	n	$E_n^{tb}(MeV)$	n	$E_n^{tb}(MeV)$
0	-75.166	6	-59.531	12	-29.605
1	-73.915	7	-55.373	13	-23.607
2	-72.022	8	-50.855	14	-17.386
3	-69.585	9	-45.998	15	-10.971
4	-66.666	10	-40.823	16	-4.402
5	-63.304	11	-35.351		

The quasi-bound energy eigenvalues given by Equation 5 and Equation 6 satisfy

$$0 < E_n^{qb} < V_0 \frac{(1-aL)^2}{4a} \tag{18}$$

i.e. $0 < E_n^{qb} < 22.705 MeV$, which are given in Table 2.

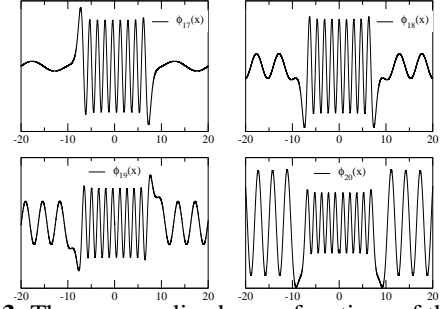**Table 2.** The quasi-bound energy spectrum of the α particle confined in Bohrium 270 nucleus.

n	$E_n^{qb}(MeV)$
17	$2.263 - 0.537 \times 10^{-3}i$
18	$8.929 - 0.146 \times 10^{-1}i$
19	$15.439 - 0.133i$
20	$21.688 - 0.650i$

Note that the tight-bound states are considered stationary, since their energy eigenvalues are real with infinite time constants. Contrarily, energy eigenvalues of quasi-bound states have complex form in general, giving rise to a finite time constant and a non-zero decay probability [49, 50].

The first two and the last two bound state wave functions are given in Figure 2, and all the quasi-bound wave functions are shown in Figure 3. The wave functions of the quasi-bound states have oscillations outside the well, indicating the α decay. Note that all the wave functions are unnormalized.
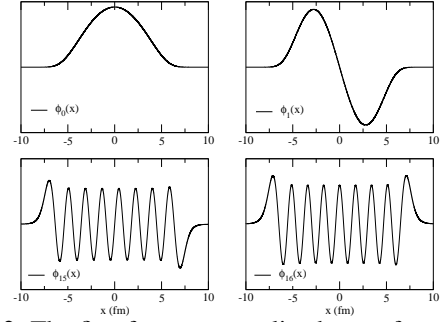
Figure 2. The first four unnormalized wave functions of the

Figure 3. The unnormalized wave functions of the quasi-bound states and the oscillations outside the well.

3.1. Thermodynamic functions of the system

We first calculate the partition function by using the energy spectrum of the system;

$$Z(\beta) = \sum_{n=0} e^{-\beta E_n}, \tag{19}$$

Here β is defined by

$$\beta = \frac{1}{k_B T}. \tag{20}$$

where k_B indicates the Boltzman constant and T is the temperature in Kelvin. The Helmholtz function of the system is calculated via the relation,

$$F(T) \equiv -k_B T \ln Z(\beta). \tag{21}$$

The entropy of the system is calculated using,

$$S(T) = -\frac{\partial}{\partial T} F(T). \tag{22}$$

The Helmholtz free energy and the entropy functions for both quasi-bound states included and excluded of the system versus the reduced temperature are seen in Figure 4(a) and Figure 4(b), respectively. The reduced temperature is defined as the unitless quantity $k_B T / mc^2$. The zero entropy at zero Kelvin is consistent with the third law of thermodynamics. The entropy saturates to the value $2.33 \times 10^{-4} eV/K$ when only the bound states are included in the partition function. When the quasi-bound states are taken into account, the number of microstates available to the system increases and the entropy saturates to a higher value, $2.96 \times 10^{-4} eV/K$ and the Helmholtz free energy decreases for high temperatures as seen in Figure

4(a). According to the behavior of entropy function, the system favours the addition of quasi-bound states, being consistent with the second law of thermodynamics. This verifies the necessity of the surface interactions.
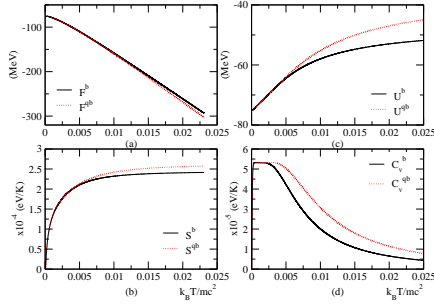
Figure 4. (a) Helmholtz free energy, (b) entropy, (c) internal energy, (d) specific heat capacity versus reduced temperature $k_B T/mc^2$. Quasi bound states are included in the red curve, excluded in the black. The saturation value of the internal energy is $-46.739 MeV$ without quasi bound states, and $-35.535 MeV$, when they are included.

The internal energy $U(T)$ is the expectation value of the energy of the α particle. It is given by

$$U(T) \quad = \quad -\frac{\partial}{\partial \beta} \ln Z(\beta). \qquad (23)$$

Then, the specific heat capacity $C_v(T)$ is

$$C_v(T) \quad \equiv \quad \frac{\partial}{\partial T} U(T). \qquad (24)$$

For the cases that the quasi-bound states are included and excluded, the plots of $U(T)$ and $C_v(T)$ are shown in Figure 4(c) and Figure 4(d), respectively.

The initial behavior of the internal energy and the specific heat against the reduced temperature are presented in Figure 5. The initial value of the internal energy at $0K$ is $-74.995 MeV$, the lowest energy eigenvalue in the spectrum. The internal energy has an initial convex increase until the reduced temperature of 2×10^{-4} followed by a linear ascent. The linear increase of the internal energy is followed by a concave ascent up to the saturation, which is $-46.739 MeV$ when the quasi-bound states are excluded, and $-35.535 MeV$ when they are included. These saturations are the mean values of the respective energy spectra. This is a consequence that, as temperature goes to infinity, all Boltzmann factors approach to unity. In this temperature regime, thus occupation of all energy values become equally probable in the spectrum.

In the linear regime, the specific heat remains constant at about $5.35 \times 10^{-5} eV/K$. When the quasi-bound are presented in the spectrum, the specific heat goes to zero in a wider temperature range.

A particle having the energy that coincides the quasi-bound energy spectrum after the tunneling into a nucleus
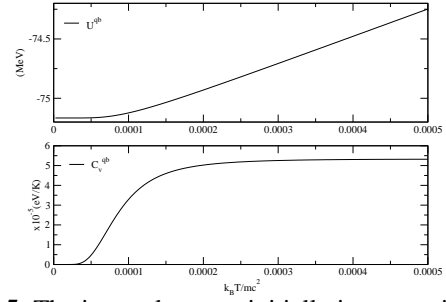
Figure 5. The internal energy initially increases in a convex manner followed by a linear ascent.

is known as the resonance. In our problem the resonance is satisfied for the α particle to decay, when it has a quasi-bound energy as indicated in Figure 6. The kinetic energy of the decayed α particle has been calculated as the mean value of the quasi-bound energy spectrum as $12.079 MeV$, which is in reasonable agreement with the experimental data [51].
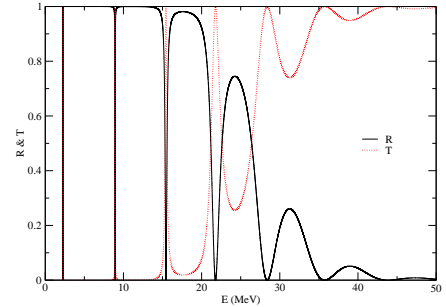
Figure 6. Transition (T) and reflection (R) coefficients of an α particle through the energy barrier at the surface, as functions of the energy.

4. Discussion and Conclusion

In this work, we revealed the contribution of the surface term added to WSP to form GSWSP, to the physics of a Bohrium 270 nucleus, in context of thermodynamic point of view. We solved the Schrödinger equation considering an α particle in a GSWSP, which has surface terms in addition to the WSP. The energy spectrum and the corresponding wave functions of the system were calculated as well as entropy, internal energy, Helmholtz energy, and specific heat, as functions of reduced temperature, using the partition functions based on the energy spectrum.

When the quasi-bound states are taken into account, the internal energy increases, while the Helmholtz energy decreases in comparison with the case of bound states solely. With this inclusion, the entropy also increases and the specific heat capacity sails at higher values, decaying to zero at longer temperature scale. The bound state wave functions imply that the nucleon is completely restricted within the nucleus, with zero decay probability, while decay probabilities have resonances leading to very high tunneling probabilities for quasi-bound states. The imaginary parts of the quasi-bound energy eigenvalues are used to calculate the kinetic energy of the decayed α parti-

cle, being in reasonable agreement with the experimental data. The difference from the experimental data is because of that the other effects such as spin-orbit coupling, orbital contribution were ignored, which reduces the original problem into one-dimensional one.

Acknowledgment

References

[1] Pacheco, M. H., Landim, R. R., Almeida, C. A. S. 2003. One-dimensional Dirac oscillator in a thermal bath. Physics Letters A, 311(2003), 93-96.

[2] Pacheco, M. H., Maluf, R. V., Almeida, C. A. S. 2014. Three-dimensional Dirac oscillator in a thermal bath. EPL, 108(2014), 10005.

[3] Franco-Villafañe, J. A., Sadurní, E., Barkhofen, S., Kuhl, U., Mortessagne, F., Seligman, T. H. 2013. First Experimental Realization of the Dirac Oscillator. Physical Review Letters, 111(2013), 170405.

[4] Boumali, A. 2015. The One-dimensional Thermal Properties for the Relativistic Harmonic Oscillators. Electronic Journal of Theoretical Physics, 12(2015), 121-130.

[5] Boumali, A. 2015. Thermodynamic properties of the graphene in a magnetic field via the two-dimensional Dirac oscillator. Physica Scripta, 90(2015), 045702, (109501 Corrigendum).

[6] Boumali, A. 2015. Thermal Properties of the One-Dimensional Duffin–Kemmer–Petiau Oscillator Using Hurwitz Zeta Function. Zeitschrift für Naturforschung A, 70(2015), 867-874.

[7] Arda, A., Tezcan, C., Sever, R. 2016. Klein–Gordon and Dirac Equations with Thermodynamic Quantities. Few-Body Systems, 57(2016), 93-101.

[8] Dong, S. H., Lozada-Cassou, M., Yu, J., Jimenez-Angeles, F., Rivera, A. L. 2007. Hidden Symmetries and Thermodynamic Properties for a Harmonic Oscillator Plus an Inverse Square Potential. International Journal of Quantum Chemistry, 107(2007), 366-371.

[9] Woods, R. D., Saxon, D. S. 1954. Diffuse Surface Optical Model for Nucleon-Nuclei Scattering. Physical Review, 95(1954), 577-578.

[10] Zaichenko, A. K., Ol'khovskii, V. S. 1976. Analytic Solutions of the Problem of Scattering by Potentials of the Eckart Class. Theoretical and Mathematical Physics, 27(1976), 475-477.

[11] Perey, C. M., Perey, F. G., Dickens, J. K., Silva, R. J. 1968. 11−MeV Proton Optical-Model Analysis. Physical Review, 175(1968), 1460-1475.

[12] Schwierz, N., Wiedenhöver, I., Volya, A. 2007. Parameterization of the Woods-Saxon Potential for Shell-Model Calculations. https://arxiv.org/pdf/0709.3525v1.pdf (Erişim Tarihi 31.01.2017).

[13] Michel, N., Nazarewicz, W., Ploszajczak, M., Bennaceur, K. 2002. Gamow Shell Model Description of Neutron-Rich Nuclei. Physical Review Letters, 89(2002), 042502.

[14] Michel, N., Nazarewicz, W., Ploszajczak, M. 2004. Proton-neutron coupling in the Gamow shell model: The lithium chain. Physical Review C, 70(2004), 064313.

[15] Esbensen, H., Davids, C. N. 2000. Coupled-channels treatment of deformed proton emitters Physical Review C, 63(2000), 014315.

[16] Brandan, M. E., Satchler, G. R. 1997. The interaction between light heavy-ions and what it tells us. Physics Reports, 285(1997), 143-243.

[17] Satchler, G. R. Heavy-ion scattering and reactions near the Coulomb barrier and "threshold anomalies". Physics Reports, 199(1991), 147-190.

[18] Kennedy, P. 2002. The Woods–Saxon potential in the Dirac equation. Journal of Physics A: Mathematical and General, 35(2002), 689-698.

[19] Panella, O., Biondini, S., Arda, A. 2010. New exact solution of the one-dimensional Dirac equation for the Woods–Saxon potential within the effective mass case. Journal of Physics A: Mathematical and Theoretical, 43(2010), 325302.

[20] Aydoğdu, O., Arda, A., Sever, R. 2012. Effective-mass Dirac equation for Woods-Saxon potential: Scattering, bound states, and resonances. Journal of Mathematical Physics, 53(2012), 042106.

[21] Guo, J. Y., Sheng, Z. Q. 2005. Solution of the Dirac equation for the Woods–Saxon potential with spin and pseudospin symmetry. Physics Letters A, 338(2005), 90–96.

[22] Guo, J. Y., Zheng, F. X., Fu-Xin, X. 2002. Solution of the relativistic Dirac-Woods-Saxon problem. Physical Review A, 66(2002), 062105.

[23] Rojas, C., Villalba, V. M. 2005. Scattering of a Klein-Gordon particle by a Woods-Saxon potential. Physical Review A, 71(2005), 052101.

[24] Hassanabadi, H., Maghsoodi, E., Zarrinkamar, S., Salehi, N. 2013. Scattering of Relativistic Spinless Particles by the Woods–Saxon Potential. Few-Body Systems, 54(2013), 2009-2016.

[25] Yazarloo, B. H., Mehraban, H. 2016. The Relativistic Transmission and Reflection Coefficients for Woods–Saxon Potential. Acta Physica Polonica A, 129(2016), 1089-1092

[26] Chargui, Y. 2016. Effective Mass and Pseudoscalar Interaction in the Dirac Equation with Woods–Saxon

Potential. Few-Body Systems, 57(2016), 289-306.

[27] Pahlavani, M. R., Alavi, S. A. 2012. Solutions of Woods–Saxon Potential with Spin-Orbit and Centrifugal Terms through Nikiforov–Uvarov Method. Communications in Theoretical Physics, 58(2012), 739-743.

[28] Costa, L. S., Prudente, F. V., Acioli, P. H., Soares Neto, J. J., Vianna, J. D. M. 1999. A study of confined quantum systems using the Woods-Saxon potential. Journal of Physics B: Atomic, Molecular and Optical Physics, 32(1999), 2461-2470.

[29] Flügge, S. 1994. Practical Quantum Mechanics. Springer, Berlin, 287s.

[30] Niknam, A., Rajabi, A. A., Solaimani, M. 2016. Solutions of D-dimensional Schrodinger equation for Woods–Saxon potential with spin–orbit, coulomb and centrifugal terms through a new hybrid numerical fitting Nikiforov–Uvarov method. Journal of Theoretical and Applied Physics, 10(2016), 53-59.

[31] Candemir, N., Bayrak, O. 2014. Bound states of the Dirac equation for the generalized Woods–Saxon potential in pseudospin and spin symmetry limits. Modern Physics Letters A, 29(2014), 1450180.

[32] Bayrak, O., Aciksoz, E. 2015. Corrected analytical solution of the generalized Woods-Saxon potential for arbitrary ℓ states. Physica Scripta, 90(2015), 015302.

[33] Bayrak, O., Sahin, D. 2015. Exact Analytical Solution of the Klein-Gordon Equation in the Generalized Woods-Saxon Potential. Communications in Theoretical Physics, 64(2015), 259-262.

[34] Lütfüoğlu, B. C., Akdeniz, F., Bayrak, O. 2016. Scattering, bound, and quasi-bound states of the generalized symmetric Woods-Saxon potential. Journal of Mathematical Physics, 57(2016), 032103.

[35] Liendo, J. A., Castro, E., Gomez, R., Caussyn, D. D. 2016. A Study of Shell Model Neutron States in $^{207;209}Pb$ Using the Generalized Woods-Saxon plus Spin-Orbit Potential. International Journal of Modern Physics E, 225(2016), 1650055.

[36] Berkdemir, C., Berkdemir, A., Sever, R. 2005. Polynomial solutions of the Schrödinger equation for the generalized Woods-Saxon potential. Physical Review C, 72(2005), 027001, errata 74(2006), 039902(E).

[37] Badalov, V. H., Ahmadov, H. I., Ahmadov, A. I. 2009. Analytical solutions of the Schrödinger equation with the Woods-Saxon potential for arbitrary ℓ state. International Journal of Modern Physics E, 18(2009), 631-642.

[38] Gönül, B., Köksal, K. 2007. A note on the Woods-Saxon potential. Physica Scripta, 76(2007), 565-570.

[39] Koura, H., Yamada, M. 2000. Single-particle potentials for spherical nuclei. Nuclear Physics A, 671(2000), 96-118.

[40] Çapak, M., Petrellis, D., Gönül, B., Bonatsos, D. 2015. Analytical solutions for the Bohr Hamiltonian with the Woods–Saxon potential. Journal of Physics G: Nuclear and Particle Physics, 42(2015), 95102.

[41] Çapak, M., Gönül, B. 2016. Remarks on the Woods-Saxon Potential. Modern Physics Letters A, 31(2016), 1650134.

[42] Ikot, A. N., Akpan, I. O. 2012. Bound State Solutions of the Schrödinger Equation for a More General Woods–Saxon Potential with Arbitrary $\ell-$state. Chinese Physics Letters, 29(2012), 090302.

[43] Ikhdair, S. M., Falaye, B. J., Hamzavi, M. 2013. Approximate Eigensolutions of the Deformed Woods–Saxon Potential via AIM. Chinese Physics Letters, 30(2013), 020305.

[44] Kobos, A. M., Mackintosh, R. S. 1982. Evaluation of model-independent optical potentials for the $^{16}O+^{40}Ca$ system. Physical Review C, 26(1982), 1766-1769.

[45] Boztosun, I. 2002. New results in the analysis of $^{16}O+^{28}Si$ elastic scattering by modifying the optical potential. Physical Review C, 66(2002), 024610.

[46] Boztosun, I., Bayrak, O., Dagdemir, Y. 2005. A Comparative Study of the $^{12}C+^{24}Mg$ System with Deep and Shallow Potentials. International Journal of Modern Physics E, 14(2005), 663-673.

[47] Kocak, G., Karakoc, M., Boztosun, I., Balantekin, A. B. 2010. Effects of $\alpha-$ cluster potentials for the $^{16}0+^{16}O$ fusion reaction and S factor. Physical Review C, 81(2010), 024615.

[48] Dapo, H., Boztosun, I., Kocak, G., Balantekin, A. B. 2012. Influence of long-range effects on low-energy cross sections of He and HeX: The lithium problem. Physical Review C, 85(2012), 044602.

[49] Gamow, G. 1928. Zur Quantentheorie des Atomkernes. Zeitschrift für Physik, 51(1928), 204-212.

[50] Siegert, A. F. J. 1939. On the Derivation of the Dispersion Formula for Nuclear Reactions. Physical Review, 56(1939), 750-752.

[51] Dunford C. L., Burrows T. Q. 1985 Online Nuclear Data Service, Report IAEA-NDS-150 (NNDC Informal Report NNDC/ONL-95/10), Rev. 95/10 (1995)9, International Atomic Energy Agency, Vienna, Austria